INFLUENCE OF SURFACE STRUCTURE ON FURFURAL CONVERSION: COMPARATIVE STUDIES ON Ni(111) AND NiO(111) SINGLE CRYSTAL SURFACES

A. Bikogiannakis[1], F. Xydas[1], A. Stylla[1], S. Tsatsos[1], G. Kyriakou[1,*]

[1]Department of Chemical Engineering, University of Patras, Patras, Greece

(*kyriakg@*upatras.gr*)

ABSTRACT

The utilization of biomass for the co-production of sustainable fuels and chemicals has the power to transform global energy and materials markets. This necessitates the development of new catalytic processes capable of selectively transforming highly functionalized organic molecules into either 'drop in' chemical intermediates and fuels, or entirely to new products with novel properties. The hydrogenation of furfural is a hot topic, and much information has already been learned towards the different reaction pathways and their dependance on electronic interactions and surface structure for atmospheric pressure and in elementary studies under Ultra high vacuum (UHV) conditions. Here, we have studied the adsorption and reactivity of furfural on Ni(111) and NiO(111) single crystal surfaces under UHV conditions, employing Temperature Programmed Desorption/Reaction (TPD/TPSR) and X-Ray Photoelectron Spectroscopy (XPS). Our findings reveal that pristine Ni(111) selectively favors propene formation from furfural, suggesting a pathway involving hydrogenation and subsequent carbon-carbon bond cleavage facilitated, in contrast with NiO(111), which exhibits negligible propene production. Interestingly, the formation of an oxide layer seems to protect against catalyst deactivation by carbon deposition, where active sites for carbon deposition are occupied by oxygen. These insights into the surface-dependent catalytic behavior of nickel surfaces provide valuable guidelines for designing more effective and stable catalysts for biomass conversion. They underscore the importance of surface composition and structure in determining catalytic performance, with potential implications for industrial applications in sustainable chemistry.

KEYWORDS: Furfural, Nickel, XPS, Catalysis, Surface

INTRODUCTION

Due to the detrimental environmental impact of fossil fuels, there's a growing need to identify and develop alternative energy sources. This has brought renewed focus on catalysis and nanotechnology, particularly on the adsorption and reactivity of highly functionalized hydrocarbons with metal surfaces. By exploring how these hydrocarbons interact with metal surfaces, the scientific community aims to design more efficient catalytic processes that can contribute to a sustainable future.[1]

Therefore, in recent years, the production of biofuels and chemicals from lignocellulosic biomass derived from agricultural waste and forestry products has attracted considerable scientific interest. Lignocellulosic biomass can be used to obtain a wide variety of useful products. In this respect, furfural is a promising renewable platform compound, obtainable via the acid-catalyzed hydrolysis of C_5 sugars such as xylans and xylose. A range of value-added fuels and chemicals can be produced from furfural such as furfuryl alcohol, furan and 2-methylfuran etc, by various reaction pathways such as hydrogenation, hydrodeoxygenation (HDO) and decarbonylation. [2-4]

The effect of bimetallic catalysts, in combination with active metal effect and support effect have been previously studied for furfural conversion. When comparing SiO_2 based catalysts, furfuryl

alcohol was produced on Cu catalysts while no product from the decomposition of the furan ring was observed. On Pd catalysts, furan was produced, whereas on Ni catalysts, ring-opening products such as higher alkanes and alcohols were produced in significant amounts. The interaction between the carbonyl group of furfural was also important in controlling the pathways, with the activation of the above mentioned group leading to the production of furfuryl alcohol and 2-methylfuran. In general, catalytic surfaces with strong oxophilicity were proposed to promote the cleavage of the C–O/C=O bond. [1,3-7]

He et al.[8] studied NiO particles towards furfural hydrogenation and showed that they can significantly convert furfural at temperatures of 423 K, while initial catalyst activity was shown to be regeneratable by calcination in air. In the present work, the oxidation of a Ni(111) surface was applied for the elementary study of the reactivity of the surface towards furfural adsorption and decomposition, at temperatures where NiO is stable in UHV conditions.

METHODOLOGY

Experiments were conducted in a UHV chamber described in detail elsewhere.[2] Briefly, the system was operated at 5 x 10^{-10} mbar, using a Ni(111) single crystal (Mateck). The crystal could be conductively cooled using liquid nitrogen to 170 K and resistively heated to a maximum temperature of 1050 K. The UHV chamber was equipped with XPS and Ultraviolet Photoelectron Spectroscopy (UPS) systems as well as an Ar^+ sputtering gun, a Quadrupole Mass Spectrometer (QMS) and a Low Energy Electron Diffraction (LEED) system. The surface was cleaned by several rounds of oxygen annealing at 800 K for 30 mins, Ar^+ sputtering (3 kV, 5 mA) at 500 K, followed by a final annealing round at 1000 K for 1 hr. Surface cleanliness was ensured by XPS and LEED. XPS spectra were acquired with 12 kV anode potential, 2.55 A filament current and 20 mA emission current with a non-monochromatic Alka excitation source (1486.6 eV). UPS measurements were performed using He(I) radiation (21.2 eV). Furfural (Sigma-Aldrich, 99%) was further purified by repeated freeze-thaw cycles and delivered onto the sample via a leak valve by backfilling the chamber to the required pressure. All doses are quoted in Langmuir (L) units (1 L = 10^{-6} torr s). Oxidation of the Ni (111) surface was performed at 493 K, while exposure to CO was performed at 253 K and to Furfural at 173 K.

RESULTS AND DISCUSSION

The adsorption and reactivity of oxygen on metal surfaces has been the subject of numerous studies over the years. Concerning Ni surfaces, it has been shown that oxygen adsorbs dissociatively at room temperature. Upon annealing the sample, or exposing it to oxygen at higher temperatures leads to the formation of a nickel oxide layer.[9] In the present work, Ni(111) was exposed to O_2 at 493 K, creating an oxide layer, the evolution of which was monitored with XPS and UPS as shown in Fig. 1. The Ni $2p_{3/2}$ (Fig. 1(a)) spectrum consists of the main peak at 852.8 eV and two plasmon loss peaks at 856.5 and 858.8 eV. [10] After exposure to 310 L O_2, the main peak, as well as the satellite features, appear significantly broadened and shifted to higher binding energies. The O 1s peak (Fig. 1(b)) centered at 530 eV, corresponds to the metal oxide, while the peak at 532.4 eV corresponds to surface hydroxyl groups, which are most likely present due to some background hydrogen gas present in the UHV system. Both peaks grow in intensity with increasing exposure to O_2. UP Spectra, shown in Fig. 1(c), are well aligned with the XPS measurements. Increasing the oxygen exposure leads to the growth of the O 2p and the Ni^{2+} 3d states with the simultaneous decline in the intensity of the metallic state of Ni 3d. Using XPS Multiquant,[11] a relation was derived between the O 1s and Ni $2p_{3/2}$ total intensities, allowing for the calculation of the thickness of the oxide layer on the surface, which in turn was compared to the lattice constant of single crystal NiO at 0.417 nm and yielded the monolayers of the oxide layer (Fig. 1(d)). The oxide layer appears to have reached a

saturation above 200 L oxygen exposure, in close approximation with previous studies on nickel oxide.[9]

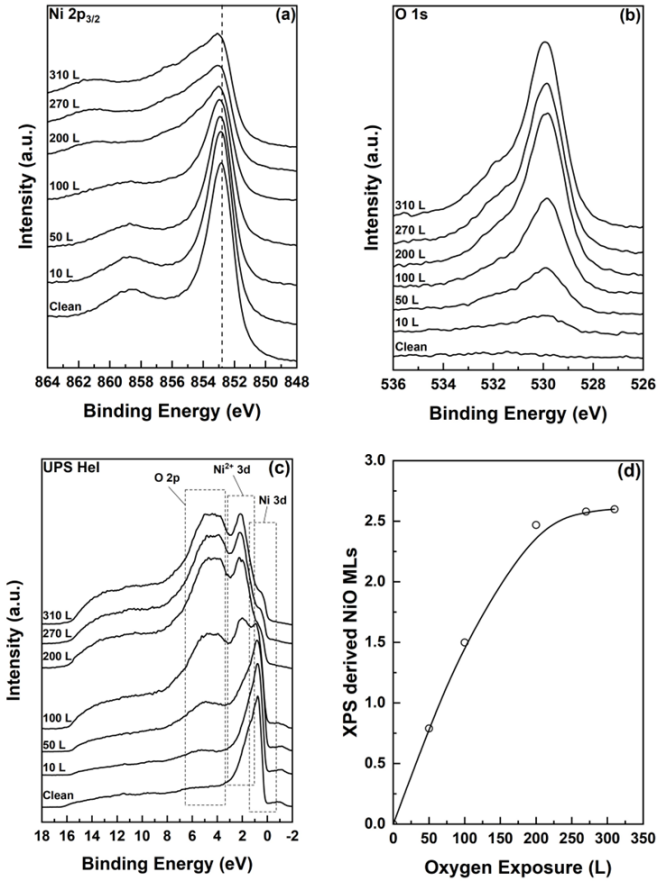

Figure 1. *Evolution of the: (a) Ni2p3/2, (b) O 1s, (c) UPS HeI spectra and (d) XPS calculated oxide monolayers formed by exposure to Oxygen.*

The growth of the oxide layer on Ni(111) has been proposed to proceed by island growth and spreading of these islands towards full surface coverage, followed by lateral oxide growth to a saturation coverage of ca. 3 ML, resulting in a well defined surface. LEED patterns show the formation of a p($\sqrt{3}$x$\sqrt{3}$) R30^{O} structure at oxygen coverages of ca. 0.5 ML, as previously reported in the literature.[12] Moreover, upon complete formation of a surface NiO layer, the LEED pattern returns to one similar to the clean surface (111). Interestingly, beyond 500 K the surface oxide layer appears to decompose. In previous work, NiO islands have been proved to be present on the surface of Ni(111) at temperatures above 690 K.[13] In this work, it is shown that oxide species can be present at temperatures up to 800 K.

The oxidation of the nickel surface was further studied towards its interaction with CO via CO TPD experiments, following exposure to carbon monoxide at 253 K, with a heating rate of 1 K s^{-1}. Exposure to growing amounts of CO leads to a small decrease of the desorption temperature from the crystal from 440 K to 420 K. Note that for first order desorption kinetics, the temperature where the desorption maximum occurs is expected to stay relatively unchanged.[14] The small reduction of the temperature of the desorption peak is most likely related to interactions between CO adsorbed molecules and surface packing. The apparent saturation coverage of CO on Ni(111) is 10 L. The desorption of CO from Ni(111) after 10L exposure leads to the formation of shoulder at lower temperatures. This shoulder has been previously attributed to a rapid decrease of the isosteric heat

of adsorption upon saturation of the surface.[15] Fig. 2(b) presents CO TPD spectra for a saturation dose of carbon monoxide on Ni(111) surfaces generated by pre-exposing the sample to varying amounts of oxygen at 493 K. Increasing the oxide thickness results in the decrease of the total amount of CO adsorbed on the surface as well as the formation of new desorption peaks. Here, the a-species are attributed to CO interaction with metallic nickel sites. The amount, as well as the desorption energy, of these species reduces with increasing oxygen pre-exposure up to 6 L. After this point, the formation of new CO adsorption sites becomes apparent, as new desorption states of CO become present at lower temperatures. In Figure 2(b) these new species are marked as species b and c and they are most likely associated CO adsorbing at the interface of NiO(111)/Ni(111). The stronger binding sites (b species) show a considerable decrease in desorption temperature and peak area with increasing oxide thickness. Interestingly, the desorption of c-species appears to be temperature independent and also shows a constant peak area from oxygen exposures of 10 L and above. Beyond 1 ML of NiO coverage, CO desorption is not observed suggesting that CO does not adsorb on the surface. The QMS signal for m/z: 44 was also recorded during the TPD measurements, which revealed no production of CO_2 by extraction of oxygen from the NiO layer, or by surface reaction of two CO molecules. Following the Redhead analysis for a first order desorption, the desorption energy was calculated and presented in Fig. 2(c).

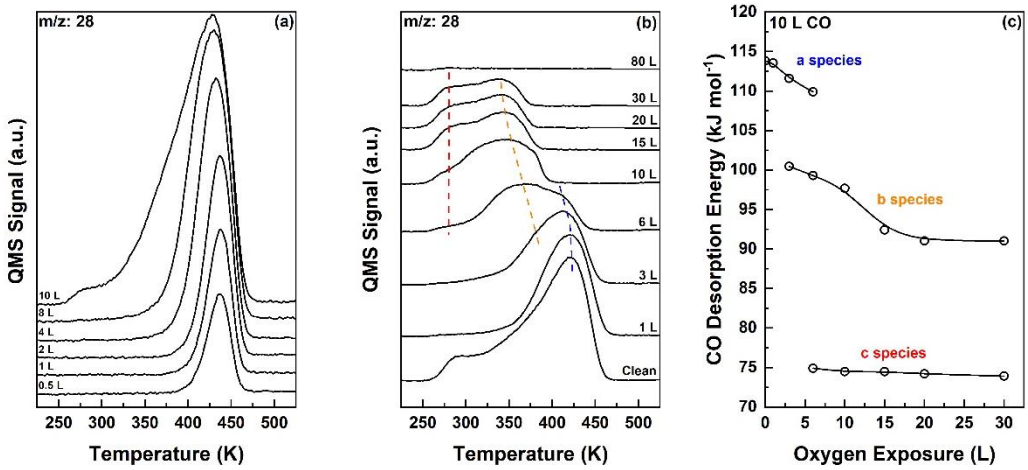

Figure 2. *(a) CO TPD from the Ni(111) surface for growing CO exposures, (b) Evolution of the CO TPD of a saturation dose at different oxygen exposures and (c) Calculated desorption energies for CO at different oxygen exposures.*

Figure 3 shows the TPSR results for furfural adsorption on the clean surface (Fig. 3(a)), from an intermediate oxide layer thickness at 0.5 ML (Fig. 3(b)) and from the NiO(111) (Fig. 3(c)) crystal surface. For the Ni(111) surface, physisorbed/multilayer furfural (m/z: 96) desorbs at 200 K with chemisorbed, unreacted furfural presenting a maximum at 225 K. Furan (m/z: 68) displays a maximum at 265 K and is formed during decarbonylation of furfural on the surface, which also produces CO (m/z: 28) that desorbs at 425 K, in accordance with chemisorbed CO on the Ni(111) surface presented earlier. 2-methylfuran (m/z: 28) is also produced on the clean Ni(111) surface and desorbs at 280 K. This product is formed through the hydrodeoxygenation (HDO) reaction pathway, consisting of hydrogenation of furfural to furfuryl alcohol, followed by C-O bond cleavage towards 2MF. Propene (m/z: 41) is produced due to C-C bond cleavage and dissolution of the aromatic ring. This species presents two maxima of QMS intensity at 280 and 325 K. Hydrogen (m/z: 2) is desorbed from the surface during dehydrogenation of remaining species and is a measure of the carbon deposition during the surface reaction. The signal of mass 39 was also recorded during the TPSR experiments as it is a common fragment for furfural, 2MF, furan and propene. It must be noted that the peaks observed for m/z: 41 and m/z: 68 at 200 and 225 K correspond to furfural, which exhibits

a fragment at these masses. For oxygen modified Ni(111), the CO signal displays a maximum at 225 K which can be attributed to the desorption of carbon monoxide produced by the decarbonylation of furfural to adsorbed furan. CO desorbed at 225 K is not chemisorbed onto the surface, but rather desorbs upon production due to the oxidation level of the surface and perhaps some surface sites, which facilitate the decarbonylation of furfural, do not facilitate the adsorption of CO. For intermediate oxide layer coverage, a desorption peak is also observed at ca. 350 K, much lower than the desorption temperature of CO from a clean Ni(111) surface, but in line with results presented earlier (see fig. 2(b)). On the saturated oxide layer, no chemisorbed CO desorption peak is observed in figure 3(c). In contrast, the rise in m/z: 28 intensity beyond 450 K, for NiO (111) is attributed to the thermal decomposition of the surface oxide layer.

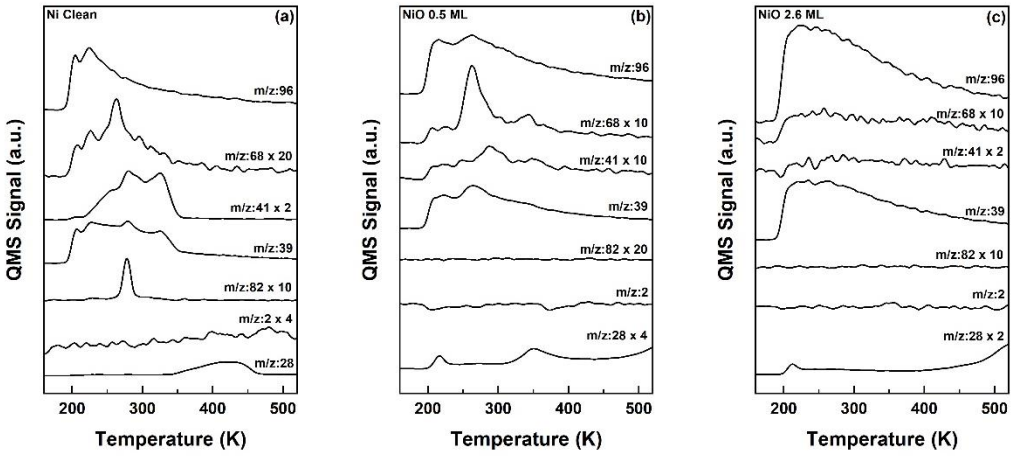

Figure 3. *Select Furfural TPD from the NiO(111)/Ni(111) surface, following exposure of a 12 L (2 ML) dose at 173 K.*

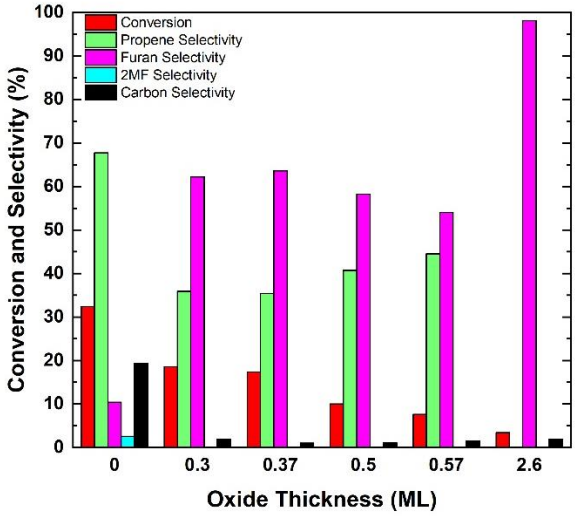

Figure 4. *Estimated conversions and selectivities for furfural TPSR on the NiO(111)/Ni(111) surface.*

The results of the TPSR experiments presented in terms of conversion and selectivity are shown in figure 4. The oxidation of the surface does not affect the desorption temperatures of the aforementioned products of the reaction, however, no production of 2MF was observed on the oxidized surface, clearly indicating inhibition of the HDO reaction pathway, which has also been reported by Jiang et al.,[7] and has been attributed to weaker interaction of the furanic ring with the surface, when decreasing oxophilicity of the surface, i.e. adding oxygen. This observation is further enhanced when considering the total furfural conversion presented in fig.4, which declines from ca.

30% to ca. 10% for 0.6 ML oxide thickness on the surface. For a saturated oxide layer, only production of furan is observed, stating that NiO(111) cannot facilitate the dissolution of the furanic ring towards propene production.

Finally, doping the surface with oxygen appears to affect carbon deposition on the catalytic surface. Notably, no H_2 desorption peak is observed for any TPSR experiment with an oxide layer on the surface, indicating minimal carbon deposition at the end of the TPD sequence. In figure 4, carbon selectivity is presented with a non-zero value due to uncertainty, however the real value does not deviate much from the presented data. It is proposed that oxidizing the surface commits active sites for carbon deposition towards the oxide layer, therefore yielding a catalyst that is durable to carbon formation. The results of this study are expected to guide the development of new Ni based materials for the selective conversion of furfural and other furanic derivatives to useful chemical products.

CONCLUSIONS

The adsorption and reactivity of CO and furfural were studied on clean and oxygen modified Ni(111) surfaces. Exposing the surface to oxygen creates an oxide layer saturated at 2.6 ML thickness at ca. 300 L exposure. CO adsorbs molecularly on Ni(111) and increasing the oxide thickness induces weaker interaction of carbon monoxide with the surface. The formation of two species attributed to CO interaction with NiO islands and NiO/Ni(111) interface are observed, with radically different desorption energies. Furfural also adsorbs non dissociatively on Ni(111) and NiO (111), and shows exponential loss of reactivity as the oxide layer thickness increases. Reaction products include propene, furan, 2MF and carbon for a clean surface, however doping the surface with oxygen yields negligible C and 2MF production. For a NiO(111) surface, only furan and CO are produced due to decarbonylation of furfural, stating inhibition of ring opening reactions and therefore negligible propene production.

ACKNOWLEDGEMENTS

Alexandros Bikogiannakis was financially supported by the “Andreas Mentzelopoulos foundation”.

REFERENCES

[1] M. J. Islam, M. Granollers Mesa, A. Osatiashtiani, J. C. Manayil, M. A. Isaacs, M. J. Taylor, S. Tsatsos, G. Kyriakou. (2021). *Appl. Catal. B: Environ. 299,* 120652.
[2] S. Tsatsos, S. Ladas, G. Kyriakou. (2020). *J. Phys. Chem. C*. 124, 26268–26278.
[3] M. J. Taylor, L. J. Durndell, M. A. Isaacs, C. M.A. Parlett, K. Wilson, A. F. Lee, G. Kyriakou. (2016). *Appl. Catal. B: Environ. 180,* 580-585.
[4] M. J. Taylor, S. K. Beaumont, M. J. Islam, S. Tsatsos, C. A. M. Parlett, M. A. Issacs, G. Kyriakou. (2021). *Appl. Catal. B: Environ.* 284, 119737.
[5] K. Xiong, J. G. Chen, (2020). *Catal. Today*. 339, 289-295.
[6] K. Xiong, W. Wan, J. G. Chen. (2016). *Surf. Sci*., 652, 91-97.
[7] Z. Jiang, W. Wan, Z. Lin, J. Xie, J. G. Chen. (2017). ACS Catal., 7, 5758-5765
[8] J. He, L. Schill, S. Yang, A. Riisager. (2018). *ACS Sustainable Chem. Eng.*, 6, 17220-17229.
[9] P. R. Norton, R. L. Tapping, G. W. Goodale. (1977). *Surf. Sci*., 65, 13-36.
[10] S. Tsatsos, G. Kyriakou (2023). *J. Phys. Chem.*, 127, 6337-6346.
[11] M. Mohai. (2004). *Surf. Interface. Anal.*, 36, 828-832.
[12] D. F. Mitchell, M. J. Graham (1982). *Surf. Sci*., 114, 546-562.
[13] D. E. A. Gordron, R. M. Lambert (1992). *Surf. Sci*., 287/288, 114-118.
[14] J. B. Miller, H. R. Siddiqui, S. M. Gates, J. N. Russell, Jr., J. T. Yates, Jr., J. C. Tully, M. J. Cardillo. (1987). *J. Chem. Phys.*, 87, 6725-6732.
[15] K. Christmann, O. Schober, G. Ertl. (1974). *J. Chem. Phys.*, 60, 4719-4724.